

HD 192163 variability revisited: A very short period WR binary or a pulsating star?*

J. M. Vreux,^{1,3} Y. Andrillat,² and E. Gosset¹

¹ Institut d'Astrophysique, Université de Liège, 5, avenue de Cointe, B-4200-Cointe-Ougrée, Belgium

² Observatoire de Haute-Provence, C.N.R.S., F-04870-St Michel l'Observatoire, France

³ Joint Institute for Laboratory Astrophysics, University of Colorado and National Bureau of Standards, Boulder, 80309, USA

Received August 31, 1984; accepted March 1, 1985

Summary. The emission line variations of HD 192163 are reinvestigated on the basis of 23 spectra collected during 15 nights spread over an interval of 20 days. The sample includes two or three observations per night during 5 nights spread over an interval of 10 days. Taking into account stratification effects in the atmosphere of the WR stars as well as the necessity of a good signal-to-noise ratio, two lines (N IV λ 4058 and N III λ 4100) have been selected for accurate position measurement. Due to the peculiar shape of the profiles, the wavelength shifts have been measured by comparing the position of every observation to a nearly noise-free profile taken as reference. The period search has been conducted using a method similar to the one of Lafler and Kinman as well as Fourier techniques. The latter includes the Discrete Fourier Transform method of Deeming as well as the Periodogram Estimate method of Scargle. The different methods all indicate that the most probable period found from the present data set is either 0.45 day or 0.31 day (these two periods are one-day aliases of each other). We cannot choose between these short periods because of the distribution of our observations. The previous period of 4.5 days suggested by earlier observers is an alias of the true period. Such a short period has never been unequivocally reported for a WR system. Either we are dealing with a deep spiral-in binary or a pulsation of a single WR star.

Key words: Wolf-Rayet stars – variable stars – close binaries – oscillations

1. Introduction

HD 192163 (=WR 136) is a WN6 star lying at the center of the "ring" nebula NGC 6888. Since it has been investigated by Koenigsberger et al. (1980) and found to show radial velocity and profile variations with a period of the order of 4.5 days, it is quoted in the literature as a WR+compact companion (Aslanov et al., 1981; Moffat, 1982, 1983). The periodicity suggested by Koenigsberger et al. (1980) was claimed to be tentative as it is based on only 10 spectra obtained with a SIT Television Camera and collected during six nights spread over an interval of 8 days. Nevertheless, that period was confirmed shortly later

* All the observations reported here have been performed with the 120 cm telescope of the Haute Provence Observatory
Send offprint requests to: J.M. Vreux (Belgium address)

by Aslanov et al. (1981) on the basis of 20 photographic spectra (IIaO; 44 \AA mm^{-1}) collected during 15 nights spread over an interval of 71 days.

In both studies, the published figures show a rather large scatter of the data around the theoretical curve. This is generally assumed to be due to the extreme difficulty of measuring radial velocity variations of the order of 10 to 30 km s^{-1} from the very broad emission lines of the WR stars (full width at half height of the order of 2000 km s^{-1}).

In both studies more than one observation per night are reported during three nights. From an inspection of the papers it appears that the difference between the radial velocities derived from observations performed during the same night is of the same order of magnitude, or even larger, as the adopted value for K , the semi-amplitude of the radial velocity variations.

From the end of August to nearly the end of September 1983 we had the opportunity to observe HD 192163 during a rather long succession of clear nights of H.P.O. The initial aim was to improve the reported period and to get a good definition of the phase for the X-ray observations by EXOSAT which were planned around mid-September. Due to some failure of the equipment, the Satellite observations were not performed. However, the analysis of the ground-based spectra proved interesting and is the subject of the present paper.

2. Observations and reductions

The plates (IIaO, baked) have been obtained at the Newtonian focus of the 120 cm telescope of Haute Provence Observatory, using the Marly spectrograph in a configuration giving a dispersion of the order of 40 \AA mm^{-1} . The reference iron spectra located on both sides of the stellar spectrum were taken with the spectrograph in the same position as for the stellar observation in order to avoid any slight effect due to any mechanical flexion (which is not known to appear in that spectrograph). As a further caution, each exposure was split into two parts. After the pointing of the star, a first exposure of the reference is made, just before the beginning of the stellar observation. A second one is made just after completion of the stellar exposure, with the telescope still pointed to the star. Each of the iron exposure is one half of the one which would be selected for an adequate density of the reference spectra.

As can be seen in Table 1, the collection of spectra we will discuss here consists of 23 spectra collected during 15 nights

Table 1. Journal of observations

<i>JD</i> 2,445,500+	Exposure time (min.)	ϕ	ΔV (km s ⁻¹)	$\Delta(0-C)$ Fe λ 4071.74 (km s ⁻¹)
77.390	162	0.20	-37	+1.2
80.342	165	0.76	6	+4.4
82.345	146	0.21	-13	+5.3
83.351	70	0.45	29	+0.4
84.455	111	0.90	4	0.0
85.429	37	0.06	-34	-3.2
86.378	135	0.17	-33	-1.3
87.360	128	0.36	32	-3.2
87.483	158	0.63	35	+2.0
88.493	61	0.87	-10	0.0
89.327	87	0.73	5	+5.7
89.385	53	0.86	10	-3.0
90.360	148	0.02	-24	-1.9
90.450	100	0.22	-11	-2.0
90.538	31	0.42	47	+2.6
91.322	75	0.16	-34	-1.2
91.367	43	0.26	-2	-1.8
91.392	18	0.32	15	+0.2
93.315	88	0.59	13	-2.1
95.380	134	0.18	-16	-1.6
96.326	69	0.28	-18	-0.9
96.394	45	0.43	12	+0.4
96.462	15	0.58	36	0.0

Note to Table 1: The phases have been calculated with $JD_0 = 2,445,580.00$ and $P = 0.45$ d. The ΔV 's given in column 3 are the mean value of the radial velocity of the group of emission lines situated around $\lambda 4060$ Å and dominated by the N IV $\lambda 4058$ and N III $\lambda 4100$ emissions (see text). The origin of the ΔV is not the rest laboratory wavelength of the lines: it is the position of the lines on the mean profile displayed in Fig. 1. The actual radial velocity of the star has been derived by Gaussian fitting of the He II lines at $\lambda 3968$ Å: this line has a reasonably unblended and symmetrical profile and originates deep in the atmosphere of the WR (Hillier, 1983). The resulting radial velocity is of the order of 13 km s^{-1} .

spread over an interval of 20 days. The reduction has been done using the facilities of the "Centre de dépouillement de clichés astronomiques", at the Nice Observatory. After digitization of the plates with the P.D.S., each spectrum has been put on a wavelength scale and an intensity scale and then normalized to the continuum. The reason of the conversion from density of intensity is that all our plates are not exposed to the same density, either on purpose (as it is impossible to get a satisfying exposure for every part of a WR spectrum on a single exposure) or due to external constraints like clouds, strong winds, The transformation from density to intensity allows one to work on more homogeneous material, specially on more "stable" profiles.

The relations used for the transformations into wavelength scales have been obtained by polynomial fitting through 15 unblended iron lines. As we were mostly interested in the blue region around $\lambda 4100$ Å (see below), 13 of these lines were situated between $\lambda 3860$ Å and $\lambda 4430$ Å. An order of magnitude

of the precision of the wavelength scales has been obtained by determining on each plate the wavelength of an iron line ($\lambda 4071.740$ Å) situated quite close to the group of WR lines we are studying. As we are interested in radial velocity variations and not in absolute values of the radial velocity what we have to look at are the variations of the residuals i.e. the variations of the difference between the observed and the laboratory wavelength of the line. The values are given in the last column of table 1. The σ is of the order of 2.5 km s^{-1} . Other iron lines give similar results. This value of σ reflects the precision which can be achieved with the spectrograph and the procedure which has been used, at least on a sharp iron line.

This uncertainty is precisely of the same order of magnitude as the variation of the heliocentric correction during the observing run. Due to the small interval of time covered by the observations, the application of the same heliocentric correction to all the data introduces a maximum error of 2.5 km s^{-1} , which is well below the precision we expect in the measurement of the broad WR lines ($\sim 10 \text{ km s}^{-1}$).

A representative spectrum of HD 192163 is displayed in Fig. 1. The low noise exhibited by the tracing is not the result of a smoothing procedure, it is the result of the addition of the 23 spectra of our collection.

Identification of the main contributor to each important feature is given as well as an indication of a second contributor when necessary (a more detailed analysis can be found in Smith and Kuhi, 1981). The He II $\lambda 4686$ line is overexposed on most of our spectra and should not be taken into consideration. Previous studies of HD 192163 have shown that there is a serious lack of homogeneity in the variations exhibited by different lines. This is most probably due to the well-known stratification of the emission lines, i.e. to the fact that with different lines we are looking at different depth in the atmosphere of the WR. This was first evidenced by the correlation of line width with ionization potential (Kuhi, 1973). For example, the lines of N IV give

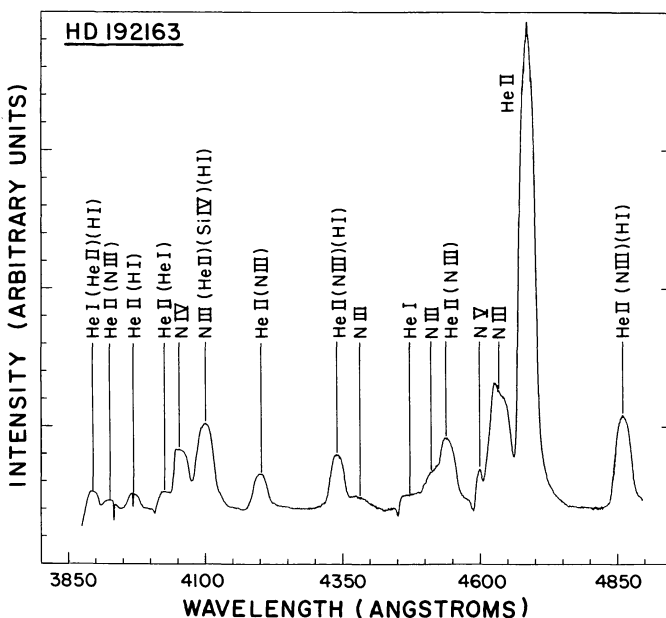


Fig. 1. Representative spectrum of HD 192163 with the identification of the main contributor(s) of the most important features. The low noise of the tracing results of the addition of 23 individual spectra

information on deeper layers than the lines of N III or most of the lines of He II.

The same applies to different lines of He II. For that ion a detailed quantitative analysis has been done recently by Hillier (1983) who has shown, for example, that the emission forming regions of He II λ 4686 and He II λ 4199 are separated by approximately $10 R_{\odot}$ in HD 50896, the latter line originating from the deepest regions.

Taking this into account as well as the fact that we also need a rather good signal-to-noise ratio and not too severe blending, the two most interesting lines are N IV λ 4058 and N III λ 4100 (see Fig. 1). Nevertheless, even for these lines the situation is not trivial if one realizes that we are looking for Doppler shift which are of the order of 1% of the total width of the line at half maximum.

To make the situation worse a careful look at the profiles show that most of them are not symmetrical and/or are more or less flat topped. A classical way to handle this kind of profile is to work on normalized tracings of the lines and to measure the position of the "center" of the line at different levels. The mean value of these measures is taken as the position of the line (Koenigsberger et al., 1980; Aslanov et al., 1981). This "manual" method allows one to use only a limited number of points on the profile, typically 3 or 4. If all the profiles under consideration were as clean as the ones displayed in Fig. 1 this method would undoubtedly give good accuracy. Nevertheless, we have to remind the reader that Fig. 1 is the result of the addition of 23 spectra and that every individual profile is much noisier. Moreover, if we look at the nice steep blue wing of N IV λ 4058, it means that we are using only 3 or 4 points to get the position while every point of the profile contains information on the true position of the line.

The problem is to take advantage of all the positional information contained within the profile without being able to rely on a mathematical expression of the profile (like for a Gaussian or a Voigt profile).

One way to proceed is to use the profile itself as a reference. A program allowing the data to be handled that way was available at the C.D.C.A. With that program the clean profiles of Fig. 1 are used as a kind of mask to which every individual spectrum is compared. This means that the program slowly shifts the individual spectrum under consideration until it gets the best fit between the individual profile and the reference profile inside a predetermined "window". This is done by minimizing an expression of the type

$$\sum_{i=1}^N (O_{\lambda_i \pm \Delta\lambda}^J - R_{\lambda_i})^2 / N$$

where O_{λ}^J and R_{λ} are the observed and reference intensities at the wavelength λ ; J is a running number designing an individual spectrum. In principle, for a binary, the reference profile has to be built iteratively, i.e. after a first determination of the $\Delta\lambda^J$ of each individual spectra, a new addition of the spectra has to be performed taking into account the individual $\Delta\lambda^J$. This new addition provides the new reference.

Practically, with the small variations we have to deal with, this iterative process was not necessary. This procedure does not give us the "true" radial velocity, it only gives the Doppler shift relative to the "mask". This method has been applied to N IV λ 4058, N III λ 4100 and to the whole profile between λ 4012 Å and λ 4136 Å. This has been done on the "rough" spectra as well as on slightly smoothed spectra. The results of all these measurements were compared between each other and three

plates had to be eliminated because the difference between the $\Delta\lambda$ obtained on smoothed and nonsmoothed spectra and/or the difference between the $\Delta\lambda$ obtained from N IV or from N III or from the three lines taken together were abnormally large compared to what was observed on the other plates and were of the order (or larger) than the variations we were looking for. The 23 remaining plates are the ones listed in Table 1.

For these 23 spectra the $\Delta\lambda^J$ finally taken into consideration for the analysis are the mean value of the $\Delta\lambda^J$ obtained from N IV λ 4058, from N III λ 4100 and from the three lines between λ 4012 Å and λ 4136 Å taken together. This means that the N IV and N III lines are taken into account twice, which seems reasonable as they are much stronger than the He II+He I line. The corresponding ΔV (km s^{-1}) are listed in the third column of Table 1.

3. Period determination

As can be seen while going through the papers dealing with WR+compact companions (references can be found in Moffat, 1983), the determination of the period of these objects is often very difficult. This is due to the large errors affecting the data which are a direct consequence of the difficulties encountered for the measurements of the Doppler shifts. Two different methods have been used to derive a period from our data.

3.1. The classical periodogram

A frequently used method for a period search is the one described by Lafler and Kinman (1965) and its derivatives like the one suggested by Bopp et al. (1970). Applying such a method to our data, in the 1 day–5.5 days range, the periodogram show a broad minimum centered around 4.5 days ($\nu = 0.222 \text{ d}^{-1}$), i.e. around the period suggested by Koenigsberger et al. (1980). We then conducted a period search between 0.1 day and 1.0 day: we indeed have 3 nights with 3 observations per night and 2 nights with 2 observations per night and these 5 nights with multiple observations are clustered on an interval of 10 days. For a given night the spacing between the observations is frequently less than 0.1 day. On the periodogram a minimum more than 2 times deeper than the one around 4.5 days appears around 0.45 day ($\nu = 2.222 \text{ d}^{-1}$). Another rather deep minimum is also present around 0.31 day ($\nu = 3.222 \text{ d}^{-1}$). As can be seen these two periods are direct aliases of each other: their frequencies differ by an integer number of d^{-1} . As a matter of fact, other aliases are also present on the periodogram at $\nu = 1.222, 4.222$, etc. All these are the well-known spurious periods arising from the unescapable one-day periodicity appearing in the distribution of the observations (Lafler and Kinman, 1965).

3.2. The Fourier analysis technique

Fourier techniques can be used for the detection of periodic signals hidden in noise even in the case of unevenly spaced data. We have applied to our data the method of the DFT (Discrete Fourier Transform) described by Deeming (1975) as well as the method of the PE (Periodogram Estimate) of Scargle (1982).

The result of the first method is shown in Fig. 2. Following Deeming (1975) the square of the full amplitude of the spectral window is given for comparison in Fig. 2a while Fig. 2b represents

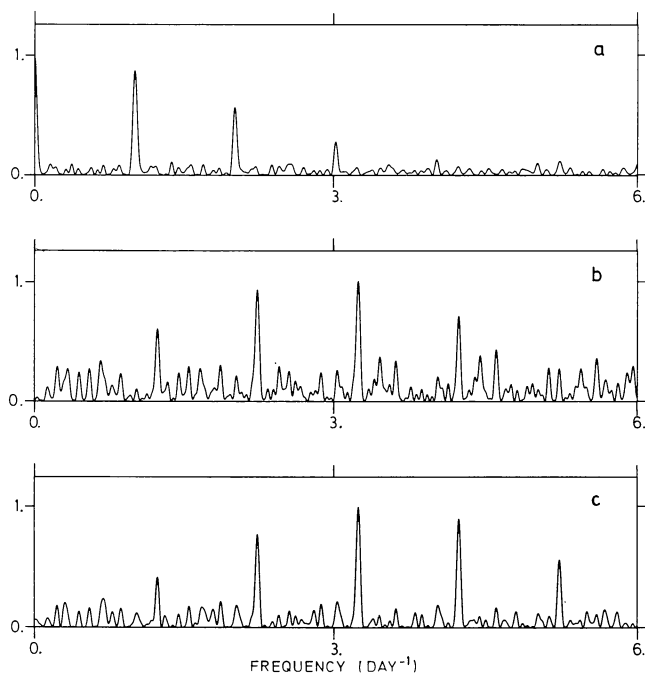


Fig. 2. Fourier analysis of the data of Table 1. (a) Square of the full amplitude of the spectral window (as defined by Deeming, 1975). (b) Square of the full amplitude of the DFT (as also defined by Deeming, 1975). (c) Square of the full amplitude of the DFT of a pure cosine monochromatic wave (see text)

the square of the full amplitude of the DFT of our data in the frequency interval $[0., 6.]$ d^{-1} . In both cases the family of one-day aliases is clearly visible. There is no doubt that a periodicity is present in the distribution of the observed radial velocities. The highest peak of the power spectrum is the most likely progenitor: it corresponds to $\nu = 3.225 \text{ d}^{-1}$ ($\sigma_\nu \approx 0.005 \text{ d}^{-1}$). Nevertheless, the noise of the data does not allow one to reject the peak at $\nu = 2.226 \text{ d}^{-1}$ ($\sigma_\nu \approx 0.005 \text{ d}^{-1}$) as the difference between the powers of the two peaks is of the order of the power of the noise. In order to have an idea of the SL (Significance Level) of these peaks we have computed the PE of our data (Scargle, 1982). The PE essentially has the same shape as the DFT with an important exception: the highest peak is the one at $\nu = 2.226 \text{ d}^{-1}$. The next one (and again the only one which can be considered as a potential candidate) is situated at $\nu = 3.225 \text{ d}^{-1}$. The SL are 0.0049 (i.e. a confidence level equal to 99.51%) and 0.0128 (i.e. a confidence level equal to 98.72%) respectively. These values of the SL confirms the existence of a periodicity in the data. The fact that the DFT and the PE do not favour the same peak is because the mathematical handling of the data is not the same. When compared to earlier methods (i.e. the DFT), the PE can show a small change in the relative amplitude of the main lobe and the quasi-alias sidelobes as mentioned by Scargle himself (1982) and illustrated in Fig. 4 of his paper. This, of course, can be critical when the two main peaks have rather similar intensities. As a matter of fact, this only points out that from our data it is not possible to make a definitive choice between the two candidates, i.e. $\nu = 3.225 \text{ d}^{-1}$ and 2.226 d^{-1} .

Figure 2c represents the DFT of a pure cosine monochromatic wave of frequency $\nu = 3.225 \text{ d}^{-1}$ sampled exactly the same way as were sampled the variations exhibited by HD 192163. There is indeed a good agreement between Fig. 2b and 2c. The same

exercise with a pure cosine monochromatic wave of frequency $\nu = 2.226 \text{ d}^{-1}$ gives a rather similar result except that the highest peak is now located at $\nu = 2.226 \text{ d}^{-1}$.

In order to check the influence of any systematic effect resulting from the observing procedure followed during the nights with multiple exposures, we have removed data points from Table 1 until we were left with only one data point per night. As expected, this new sample exhibits much stronger one day aliases. Nevertheless, the same trend remains: the peaks corresponding to frequencies higher than 1 d^{-1} show up better.

We have also investigated the data of Aslanov et al. (1981) and Koenigsberger et al. (1980) with the Fourier techniques. The first ones give rather noisy results: a periodical phenomenon is most probably present in the data but nothing can be said about the period. The results of the Fourier analysis of the data of Koenigsberger et al. (1980) for He II λ 4686 are given in Fig. 3. Figure 3a shows that the one-day aliasing is much more severe than with our data: the intensity of the peaks decreases much more slowly than in Fig. 2a. The DFT (Fig. 3b) shows a family of double peaks, one-day aliases of each other. The apparition of double peaks is most probably due to the shape of the spectral window. As can be seen, it is not possible to safely derive a period from these data: there is a peak corresponding to the 4.5 days period ($\nu = 0.222 \text{ d}^{-1}$) as well as peaks corresponding to the 0.45 day period ($\nu = 2.226 \text{ d}^{-1}$) and to the 0.31 day period ($\nu = 3.225 \text{ d}^{-1}$). All these peaks and a few other ones have nearly the same intensity, the peak corresponding to the 4.5 day periods being hardly weaker than the ones corresponding to higher frequencies. It is clear that no choice of period can be made from these data. The only information is that, from these data, the period we have found is at least as probable as the 4.5 day period. Figure 3c is the DFT of a pure cosine monochromatic wave of frequency $\nu = 3.225 \text{ d}^{-1}$ sampled exactly the same way as were the variations of HD 192163 during the observations of Koenigsberger et al. (1980).

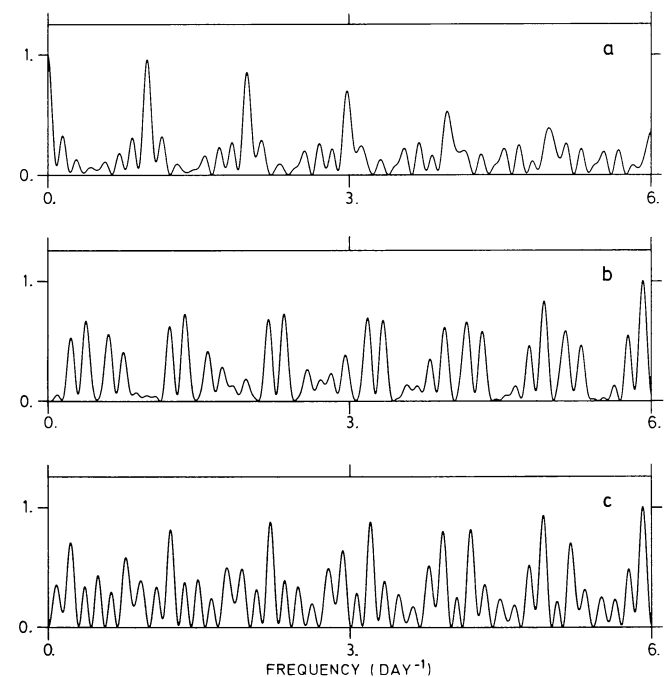


Fig. 3. Fourier analysis of the data of Koenigsberger et al. (1980). The three parts of the figure are essentially defined as in Fig. 2

As a conclusion, from this analysis of the data it looks clear that the variability exhibited by HD 192163 is periodic and that the period is either 0.45 d or 0.31 d. We have used three different methods to determine the period: two of them slightly favour the 0.45 d period. In the future, we will take that period as the best choice.

Before elaborating further, such a short period raises the methodological question of the relative lengths of exposure times and period. To evaluate the influence of the result of the exposure times which are a sizeable fraction of the period (the usual practice is to keep the exposure time less than 0.1 period) a period search has been conducted using only the data corresponding to exposure times less than respectively 0.1 P and 0.12 P. In both cases the periodograms show a very deep and well defined minimum around 0.453 day (and 0.31 day) and nothing around 4.5 days. This will be illustrated later on the graphs giving the radial velocity variations as a function of phase (Figs. 5 and 6). The net result of removing the long exposures is to improve the minimum on the periodogram, not to modify the fact that the period is around 0.45 day (or 0.310 day). The next step will be to investigate the same effect on the orbital solution: this will be done in the following section.

4. Interpretation: spiral-in or pulsation

Fitting a velocity orbit to the data of Table 1 gives a K of the order of 32 km s^{-1} and an eccentricity close to 0.28 (Aslanov, 1981, suggests $K \approx 20 \text{ km s}^{-1}$ and $e = 0.3$). The corresponding solution and the data points are plotted on a phase diagram in Fig. 4. As can be seen, the fit is reasonably good. With these orbital elements we get a mass function

$$f_{\text{mass}} = \frac{(m_2 \sin i)^3}{(m_{\text{WR}} + m_2)^2} \approx 0.0013$$

in which m_2 refers to the mass of the unseen star and i to the inclination of the orbit. This value of f_{mass} is of the same order of magnitude as the value of 10^{-2} – 10^{-3} quoted earlier by Aslanov (1981) while our period is ten times smaller: this results from our larger value for K .

To test the influence of the long exposure times on the solution, a completely independent analysis has been made using only the observations corresponding to the short exposure times as had been done for the periodograms. The result is only slightly

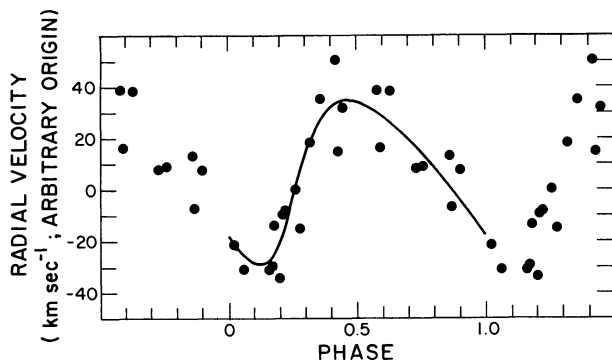


Fig. 4. Radial velocity variations as a function of orbital phase of the group of emission lines situated around $\lambda 4060 \text{ \AA}$ and dominated by the N IV $\lambda 4058$ and N III $\lambda 4100$ emissions. The continuous curve represents the theoretical radial velocities as defined by the orbital elements given in the text ($K \approx 32 \text{ km s}^{-1}$; $e \approx 0.28$)

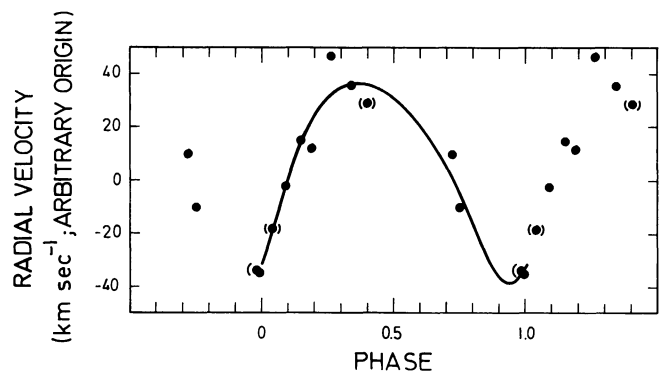


Fig. 5. Radial velocity variations as a function of orbital phase using the same lines as for Fig. 4. For the present figure we have used the result of the analysis of the data corresponding to short exposure times: the dots correspond to exposure times less than 0.045 d, the dots between brackets correspond to exposure times between 0.045 d and 0.05 d (they have been added to increase a little bit the sample while remaining close to the 0.1 period limit). The continuous curve represents the theoretical radial velocities as defined by the orbital element derived in the analysis of the short exposure times ($K = 37 \text{ km s}^{-1}$; $e = 0.25$; $P = 0.45 \text{ d}$)

different from the one reported above: K is now of the order of 37 km s^{-1} and e of the order of 0.25. The corresponding solution as well as the data points are plotted on a phase diagram in Fig. 5. As can be seen the fit is reasonably good. For comparison the same data points have been ordered according to phase using the 4.5 days period and plotted on the same type of diagram in Fig. 6. A fit with an orbital solution is obviously more difficult. The orbital elements derived using only the short exposure times give a mass function of 0.0022 which is of the same order of magnitude as the one quoted above. We will take this value 0.0022 as the most probable.

Assuming that $\sin i = 1$ and that the mass of the WR is of the order of $20 M_{\odot}$, the corresponding mass of m_2 is of the order of $1.0 M_{\odot}$ which is in the usual range of the masses quoted for neutron stars. The orbital elements also imply that the unseen companion orbits into the extended atmosphere of the WR as we get a separation between the two stars of the order of $7 R_{\odot}$ which is inferior to the radius observed in the visible by Cherepashchuk et al. (1984) in the case of the WN5 binary V 444 Cygni. It is of the order of the radius they observe in the near UV.

If the variations exhibited by HD 192163 are due to the orbital motion of an unseen companion, then we are dealing with the

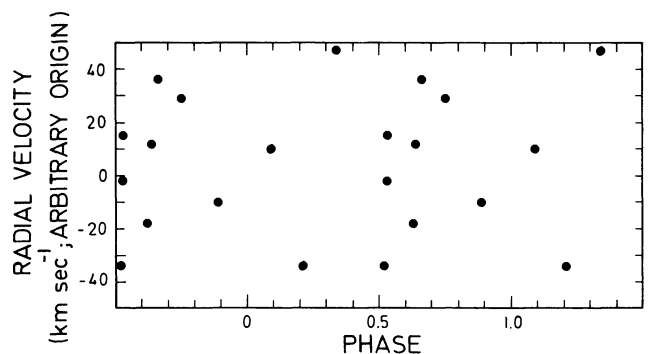


Fig. 6. The same data points as in Fig. 5 ordered according to phase using the 4.5 d period to compute the phase

first unequivocally reported case of a spiral-in binary with a period less than one day. In such a case it is, however, surprising that we get an eccentricity of the order of 0.25: due to the drag effect by the atmosphere of the WR one would expect a rather rapid circularisation of the orbit.

Nevertheless, another explanation has been suggested by Conti (1984), i.e. the variability could be due to nonradial pulsations. In that case, the reported radial velocities variations are due to profile variations of the lines, undetected as such due to an inappropriate resolution and mainly an insufficient signal-to-noise ratio.

Profile variations on a short time scale have indeed been reported as early as 1970 (Smith et al., 1970). However, in the published literature we have not found any discussion of observations of profile variations conducted in such a way that a periodicity of the order of half a day could have been put into evidence.

This kind of observation is not easy to perform: good resolution and excellent signal-to-noise ratio have to be obtained in a reasonably short time (~ 1 hour). On the other hand, periods close to half a day requests observations extending on a rather long interval of time. While the idea of nonradial pulsation is exciting a great deal of effort will be needed to check it. One of us (Vreux 1984), has investigated the radial velocity variations reported for a number of so-called WR+compact systems (Moffat, 1983) and has shown that the distribution of the published periods favours the nonradial pulsation hypothesis instead of the spiralling-in neutron star scenarios.

Acknowledgements. First of all, the generous allocation of observing time by the Haute Provence Observatory has to be acknowledged: a long observing run is a fundamental necessity for the kind of problem we had to deal with. J.M.V. would like to express his thanks to the Belgian Ministère de l'Éducation Nationale which provided support for his observing runs at the Haute Provence Observatory. The help of the night assistants of the 120 cm telescope is also gratefully acknowledged. Y.A. and J.M.V. would like to express their heartiest thanks to A. Bijaoui, head of the C.D.C.A., for the help he has provided during their two stays at the C.D.C.A., and specially for the use of his program allowing automatic measurement of wavelength shifts. The help of G. Marchal in the use of the P.D.P. and the associated program is also gratefully acknowledged. J.M.V. would also like to express his thanks to the Belgian "Académie Royale de Belgique" (Classe des Sciences) which provided some support for his first stay at

the C.D.C.A. and to the Belgian "Fonds de la Recherche Fondamentale Collective" which provided some support for the second stay. This paper has been written while one of the authors (J.M.V.) was a visitor at JILA. That stay has been possible thanks to the help of the Belgian Fonds National de la Recherche Scientifique which provided air fare and some support for the stay. The numerous facilities provided by JILA during his stay are also gratefully acknowledged. This work has benefitted by P. Conti's continuous interest which led to an appreciated improvement of the paper. This work has also benefitted of the computing facilities provided by the Centre de Calcul de l'Université de Liège. E.G. is supported by a grant of the Belgian Fonds de la Recherche Fondamentale Collective which is gratefully acknowledged. Discussions of the manuscript with Dr. Niemela have also helped to improve this paper.

References

- Aslanov, A.A., Cherepashchuk, A.M.: 1981, *Sov. Astron. Lett.* **7**, 265
- Bopp, B.W., Evans, D.S., Laing, J.D., Deeming, T.J.: 1970, *Monthly Notices Roy. Astron. Soc.* **147**, 355
- Cherepashchuk, A.M., Eaton, J.A., Khaliullin, K.F.: 1984, *Astrophys. J.* **281**, 774
- Conti, P.S.: 1984, (private communication)
- Deeming, T.J.: 1975, *Astrophys. Space Sci.* **36**, 137
- Hillier, D.: 1983, Ph.D. Thesis, Australian National University, Canberra
- Koenigsberger, G., Firmani, C., Bisiacchi, G.F.: 1980, *Rev. Mexicana Astron. Astrofiz.* **5**, 45
- Kuhi, L.V.: 1973, in *WR Binaries and Atmospheric Stratification*, IAU Symp. No. 49, eds. M.K.V. Bappu, J. Sahade, (Reidel: Dordrecht), p. 205
- Moffat, A.F.J.: 1982, in *WR Stars: Observations, Physics and Evolution*, IAU Symp. No. 99, eds. C. de Loore, A. Willis, (Reidel: Dordrecht), p. 263
- Moffat, A.F.J.: 1983, in *WR Stars: Progenitors of Supernova*, Proc. workshop Observatoire de Paris-Meudon
- Scargle, J.D.: 1982, *Astrophys. J.* **263**, 835
- Smith, L.F., Kuhl, L.V.: 1970, *Astrophys. J.* **162**, 535
- Smith, L. F., Kuhl, L.V.: 1981, An Atlas of WR Line Profiles, JILA Report No. 117
- Vreux, J.-M.: 1984, *Publ. Astron. Soc. Pacific* **97**, 274